Application of a Modular Particle-Continuum Method to Partially Rarefied, Hypersonic Flow

Timothy R. Deschenes and Iain D. Boyd

Department of Aerospace Engineering, University of Michigan, Ann Arbor, MI, USA

Abstract. The Modular Particle-Continuum (MPC) method is used to simulate partially-rarefied, hypersonic flow over a sting-mounted planetary probe configuration. This hybrid method uses computational fluid dynamics (CFD) to solve the Navier-Stokes equations in regions that are continuum, while using direct simulation Monte Carlo (DSMC) in portions of the flow that are rarefied. The MPC method uses state-based coupling to pass information between the two flow solvers and decouples both time-step and mesh densities required by each solver. It is parallelized for distributed memory systems using dynamic domain decomposition and internal energy modes can be consistently modeled to be out of equilibrium with the translational mode in both solvers. The MPC results are compared to both full DSMC and CFD predictions and available experimental measurements. By using DSMC in only regions where the flow is nonequilibrium, the MPC method is able to reproduce full DSMC results down to the level of velocity and rotational energy probability density functions while requiring a fraction of the computational time.

Keywords: hybrid methods, hypersonic flow, multiscale, DSMC, Monte Carlo, Navier-Stokes
PACS: 47.11.St, 47.40.Ki, 47.45.-n, 47.70.Nd

INTRODUCTION

Throughout their flight regime, hypersonic vehicles experience flow conditions that range from very near continuum flow to completely rarefied. Computational Fluid Dynamics (CFD) which solves that Navier-Stokes equations can be used to solve very near continuum flow conditions that are experienced at low altitudes, but these equations break down at higher altitudes due to the decrease in free stream density and the corresponding decrease in the number of collisions a particle experiences as it moves around the vehicle. The particle-based direct simulation Monte Carlo method [1] (DSMC) is well suited to solve fully rarefied flows experienced at higher altitudes, but as the density increases, the corresponding increase in range of molecular length and time scales around hypersonic vehicles that contain both a high density shock layer and low density wake, requires a large computational cost. Instead, a hybrid method can be used to maintain the physical accuracy of DSMC in regions that are rarefied, while still achieving the efficiency of CFD in regions that are considered continuum. This paper applies a hybrid MPC method to partially-rarefied, hypersonic flow over a sting-mounted planetary probe.

MODULAR-PARTICLE CONTINUUM METHOD

The MPC method [2] uses existing state of the art CFD (LeMANS) [3] and DSMC (MONACO) [4] solvers with very little modifications. Both flow solvers maintain their own mesh and data structure, and a hybrid data structure and hybrid functions are constructed to facilitate the information transfer between each flow solver.

A typical hybrid cycle progresses as follows. First, a full CFD solution and mesh is provided to the hybrid solver. An initial interface location is computed using the breakdown parameter shown in Eq. 1 which is the maximum of gradient length Knudsen numbers and a rotational nonequilibrium Knudsen number. The gradient length Knudsen number used in this work is computed for translational and rotational temperatures, mass density, and velocity magnitude. In addition, a rotational nonequilibrium breakdown parameter is applied to ensure that the rotational energy probability density function is near equilibrium within the continuum region of the flow field. For the current work, the constant, $A_{\mathrm{ROT-NEQ}}$, is set to unity. This work uses a final breakdown parameter of 0.1 such that DSMC is used when $\mathrm{Br} > 0.1$, while CFD is used elsewhere.

$$\mathrm{Br} = \max\left(Kn_{GL-Q} = \lambda \left| \frac{\nabla Q}{Q} \right|,\ Kn_{\mathrm{ROT-NEQ}} = A_{\mathrm{ROT-NEQ}} \frac{|T_{\mathrm{TRA}} - T_{\mathrm{ROT}}|}{T_{\mathrm{ROT}}} \right) \tag{1}$$

Next, an overlap region is created by extending DSMC into the initial continuum region. Then, DSMC particles are created within the rarefied portion of the flow field and particles are moved and collide using standard DSMC routines. Figure 1(a) shows a schematic of the DSMC and CFD mesh structure at the interface location during the unsteady portion of the flow simulation. DSMC particles are repopulated in boundaries at each time-step consistent with the Chapman-Enskog velocity distribution function [5] and Boltzmann rotational energy probability density function. Macroscopic quantities are tracked in DSMC cells using a subrelaxation average [6], and after the interfaces have stopped moving, DSMC information within CFD boundary cells is passed to the CFD solver and CFD cells are iterated over. Each module continues towards steady-state while information in boundaries are updated at specified intervals. Once the interface locations have stopped moving, and the flow has reached steady-state, the overlap region is removed, interfaces are locked, and DSMC sampling begins. Since the interface locations can vary throughout the unsteady period as the flow relaxes from the initial full CFD solution to the final DSMC solution, dynamic domain decomposition must be performed to maintain acceptable load balancing. At each recalculation of the interface location and between each solver switch, repartitioning of the mesh is performed to ensure that the parallel load balance is maintained [7]. In addition, the rotational relaxation models used in both flow modules are ensured to remain consistent at the continuum limit [8].

FLOW CONDITIONS

Comparison of predictions of flow over a sting-mounted, 70-degree blunted sphere cone with full DSMC, full CFD, and the MPC method is performed. The geometry and flow conditions correspond to the moderate Knudsen number experimental test case performed in the SR3 wind tunnel in Meudon, France with a probe diameter of 5 cm [9]. Table 1 summarizes the flow conditions studied in this work. Figure 1(b) shows the continuum-rarefied interface location predicted and the variation in mean free path over the planetary probe. Due to the overlap region, the interface location correctly moves to the true continuum-rarefied boundary as the MPC method progresses towards the final rarefied flow result. The large variation in flow length scales about the probe show that this test case is well suited to use to verify and validate the hybrid method.

Table 1. Experimental flow conditions for the planetary probe configuration [9].

M_∞	U_∞ [m/s]	ρ_∞ [kg/m^3]	T_∞ [K]	T_w [K]	Kn_∞
20.	1502.	5.19×10^{-5}	13.6	300.	0.01

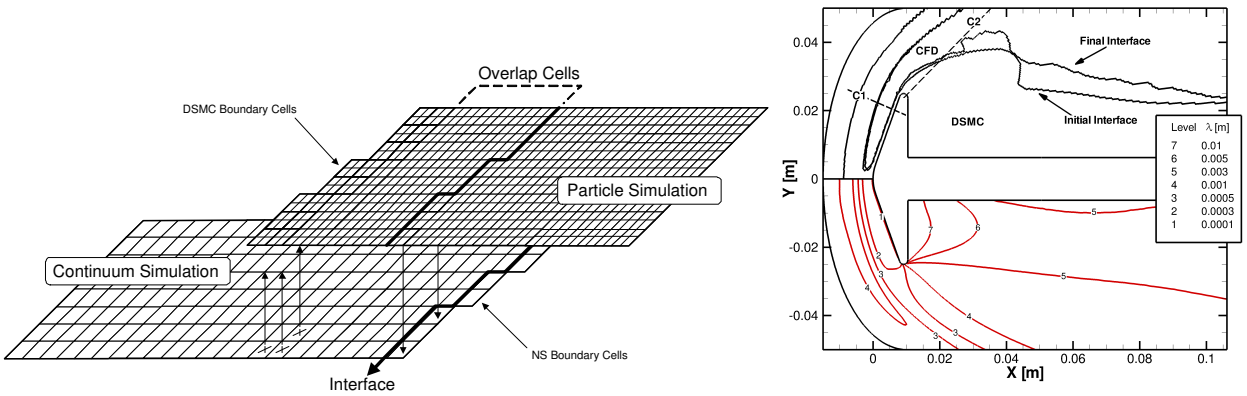

Figure 1. Schematic of the MPC mesh structure at the interface location (left); interface location and variation of mean free path around probe (right).

RESULTS

The purpose of the MPC method is to reproduce full DSMC results at a reduced computational expense. This section compares flow field, probability density functions, and surface property predictions made by full DSMC, full CFD, and the MPC method. In addition, heat surface results are compared with experimental heat transfer measurements, and the code efficiency of the MPC method compared to full DSMC and a previous MPC simulation is discussed.

Flow Field Properties

Figures 2 compare translational and rotational temperature contours predicted by full DSMC, full CFD, and the MPC method. In general the MPC method has improved agreement with full DSMC results from the initial CFD result across the entire flow field. Even in regions where the CFD module is used, the MPC method has obtained improved boundary conditions from the DSMC solver which has allowed the CFD solver to shift its result to excellent agreement with full DSMC.

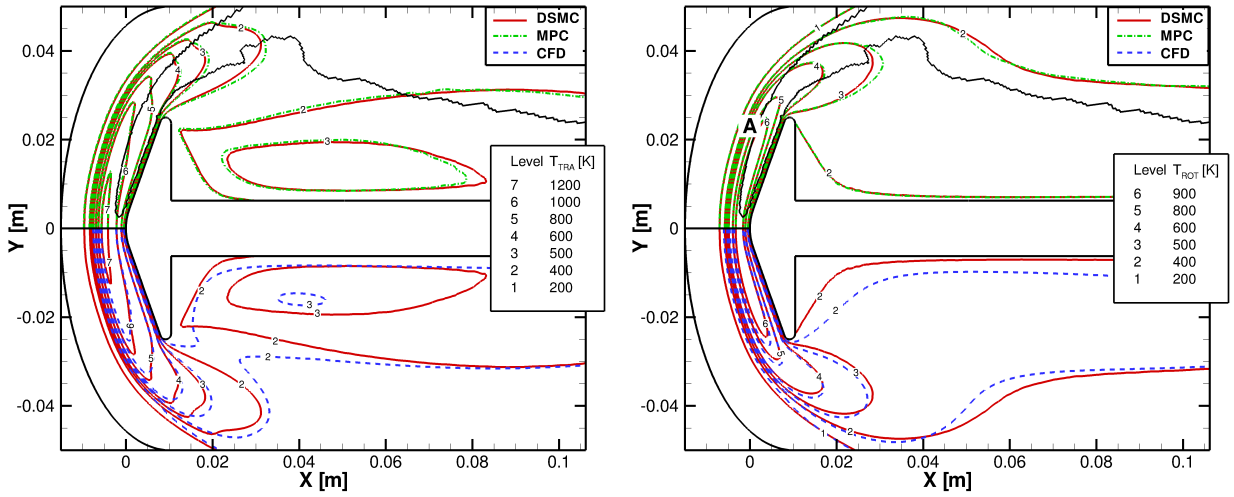

Figure 2. Comparison of translational (left) and rotational (right) temperature by DSMC, CFD, and the MPC method.

Figures 3 illustrate the prediction of flow field properties made by full DSMC, full CFD, and the MPC method along the extraction lines shown in Fig. 1(b). In addition to current MPC results, previous temperature results obtained with the MPC method using a single temperature model within the CFD solver are included[10]. To compensate for the inability to model rotational nonequilibrium within the continuum solver, this MPC simulation used a more restrictive rotational nonequilibrium parameter in compression regions of $Kn_{\mathrm{ROT-NEQ}} = 5 \times (T_{\mathrm{TRA}} - T_{\mathrm{ROT}})/T_{\mathrm{ROT}}$ [10, 2]. Vertical lines denote the interface location for the corresponding MPC result. In general, both MPC results remain in excellent agreement with the full DSMC results along C1, while the MPC simulation with rotational nonequilibrium included in CFD can simulate a larger region of the flow with CFD which directly decreases the number of DSMC particles required and increases the computational efficiency of the MPC method relative to full DSMC. Although both MPC results remain in excellent agreement with DSMC very near the surface along C2, the MPC results with a single temperature modeled within the CFD module can not accurately model the strong thermal nonequilibrium that exists along nearly the entire extraction line. In contrast, the MPC prediction with the ability of modeling a separate rotational temperature within the CFD solver remains in excellent agreement with full DSMC along the entire extraction line. Again, the DSMC region simulated using the MPC method with the ability to model rotational nonequilibrium within the CFD solver is smaller due to the less restrictive breakdown parameter.

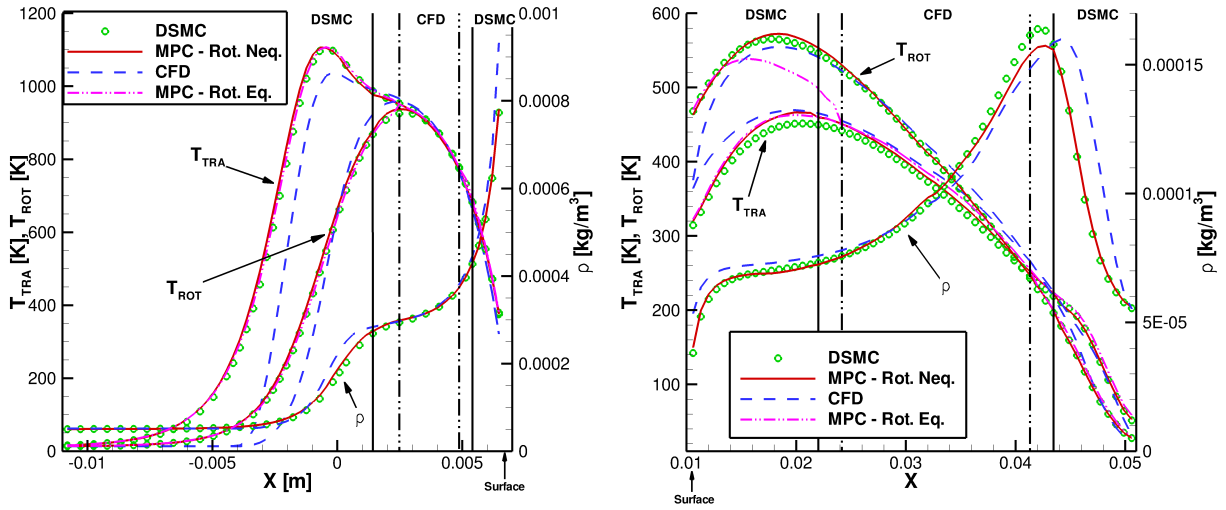

Figure 3. Temperature and density predicted by DSMC, CFD, MPC (Rot. Neq.), and the MPC method (Rot. Eq.) along C1 (left) and C2 (right).

Probability Density Functions and Surface Properties

Figures 4 compare velocity and rotational energy probability density functions predicted by full DSMC, full CFD, and the MPC method at point A shown in Fig. 2. Due to the high degree of collisional nonequilibrium within the shock, the CFD velocity distribution function which is generated from gradients and the first order Chapman-Enskog expansion does not contain sufficient information to correctly generate the velocity distribution function predicted by full DSMC. In contrast, the MPC method is able to remain in very good agreement with DSMC throughout the entire velocity space. Despite the macroscopic rotational temperature predicted by CFD to be within 5% of the full DSMC result, the rotational energy distribution function predicted by full CFD is in poor agreement with the DSMC result throughout the entire rotational energy space. Similarly to the velocity distribution function, the MPC method remains in excellent agreement with full DSMC results for the rotational energy probability density function.

Figure 5 compares the surface coefficient of heat flux, defined in Eq. 2, predicted by full DSMC, full CFD, and the MPC method with available experimental measurements.

$$C_H = \frac{q}{\frac{1}{2}\rho_\infty U_\infty^3} \tag{2}$$

Along the fore body where the flow is highly collisional, all three methods are in good agreement with each other and the experimental measurements. Despite this highly collisional flow, CFD still slightly over predicts DSMC and MPC results. This is due to the inability to correctly model the Knudsen layer within the CFD solver. As the flow expands around the corner, full CFD over predicts both DSMC and experimental measurements by over an order of magnitude. In contrast, the MPC method remains in good agreement with both the experimental measurements and the full DSMC results. Similarly, the MPC method remains in excellent agreement with full DSMC and experimental measurements along the sting mount, while full CFD over predicts full DSMC along the entire sting mount.

Computational Performance

The MPC method reproduces full DSMC results by using DSMC in rarefied regions while decreasing the computational cost by limiting DSMC to *only* regions that are in collisional nonequilibrium. Continuum regions are computed using an implicit Navier-Stokes solver that can consistently model moderate rotational nonequilibrium. Table 2 summarizes the computational performance and memory requirements of the MPC method relative to full DSMC at this

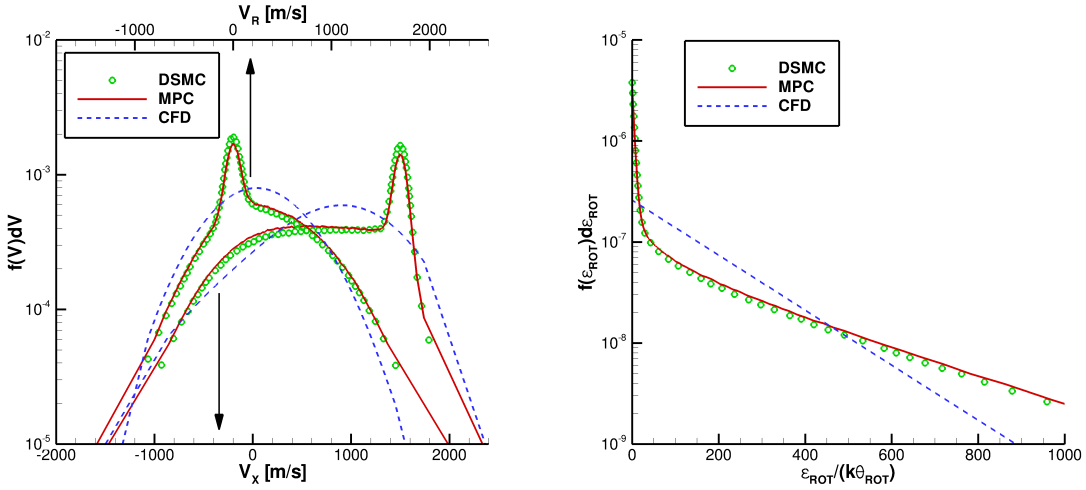

Figure 4. Comparison of velocity (left) and rotational energy (right) distribution functions predicted by DSMC, CFD, and the MPC method within the bow shock.

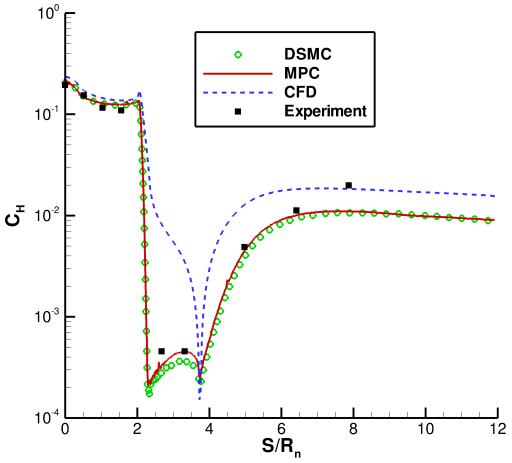

Figure 5. Surface heat transfer along planetary probe.

flow condition. For this case, the number of DSMC samples are kept constant between MPC and full DSMC simulations, while parallel efficiency was similar by setting the final number of particles on each processor to be the same for both simulations. Here, the computational cost is the ratio of total CPU time required by the MPC method to the total CPU time required by full DSMC. Ideal speedup is defined as the ratio of the total number of particles required by full DSMC to the total number of particles required by the MPC method. Despite the CFD module requiring a non-negligible amount of time within the MPC method for this test case, the ideal speedup was still exceeded due to the reduction in the number of DSMC iterations required to reach steady-state. In addition, this speedup can be compared to previous results obtained with the MPC method that used a single temperature model in the CFD module and a correspondingly more restrictive rotational nonequilibrium breakdown parameter within compression regions. Schwartzentruber et al. [10] found a relative speedup of 1.52x using a single temperature within the CFD module, while this work finds a relative speedup of 1.67x using the same mesh and DSMC parameters. In addition, it should be noted that the MPC simulation with a single temperature modeled in the continuum solver was performed in serial and did not include the corresponding parallel overhead. Despite this extra overhead, the current results still outperform

the previous results. This improved efficiency is directly due to the reduction in the number of DSMC particles required by the MPC method due to the ability to model moderate rotational nonequilibrium within the CFD solver. The overhead of solving an extra conserved equation in each CFD cell is outweighed by the decrease in computational cost of simulating less DSMC particles. The modest speedup factor achieved for this test case is a result of the fact that the flow is highly rarefied and only a small region of the flow can be simulated with the continuum module. Application of the MPC method to lower Knudsen number cases, where most of the flow can be simulated using the continuum module, have experienced higher speedup factors reaching near 30x [8, 10]. Due to both CFD and DSMC solvers using the same mesh density, the MPC method required moderately more memory compared to full DSMC.

Table 2. Computational performance and memory requirements for the MPC method.

Kn	Computational Cost (Speedup)	Ideal Speedup	Memory Usage	Initial CFD
0.01	60.% (1.67x)	1.65	130%	3.71%

CONCLUSION

The modular particle-continuum (MPC) method was described and applied to partially rarefied, hypersonic flow over a sting-mounted planetary probe configuration. This hybrid method uses existing DSMC and CFD codes with very little modifications as modules within a hybrid code. It was found that the MPC method can reproduce full DSMC results down to velocity and rotational energy distribution functions using a fraction of the computational time. Flow field results were compared between full CFD, full DSMC, and the MPC method and it was found that, even in regions where full CFD was in poor agreement, the MPC method was able to remain in excellent agreement with full DSMC. Surface heat flux predictions were compared with available experimental measurements. In the fore body, all methods remained in good agreement, while CFD greatly over predicted the surface heat flux predicted by DSMC, the MPC method, and experimental measurements by over an order of magnitude in the highly nonequilibrium wake region.

The computational performance of the MPC method relative to full DSMC was compared. By using DSMC only in regions that exhibit nonequilibrium effects, the MPC method was able to reproduce full DSMC results 1.67 times faster than full DSMC. In addition, current computational results were compared to previous results obtained using a single temperature within the continuum module. If was found that the overhead of solving an extra conserved variable in the CFD module was outweighed by the reduction in the number of DSMC particles simulated with the MPC method. This added physical modeling within the CFD solver led to both an increased agreement with full DSMC and an overall decrease in computational cost relative to previous MPC simulations.

ACKNOWLEDGMENTS

The authors gratefully acknowledge the financial support provided by the Constellation University Institute Project (CUIP) through NASA grant NCC3-989.

REFERENCES

1. G. A. Bird, *Molecular Gas Dynamics and the Direct Simulation of Gas Flows*, Clarendon Press, 1994.
2. T. E. Schwartzentruber, L. C. Scalabrin, and I. D. Boyd, *Journal of Computational Physics* **225**, 1159–1174 (2007).
3. L. C. Scalabrin, *Numerical Simulatiion of Weakly Ionized Hypersonic Flow Over Reentry Capsules*, Ph.D. thesis, University of Michigan (2007).
4. S. Dietrich, and I. D. Boyd, *Journal of Computational Physics* **126**, 328–342 (1996).
5. A. L. Garcia, and B. J. Alder, *Journal of Computational Physics* **140**, 66–70 (1998).
6. Q. Sun, and I. D. Boyd, *Journal of Thermophysics and Heat Transfer* **19**, 329–335 (2005).
7. T. R. Deschenes, T. D. Holman, and I. D. Boyd, "Parallelization of Modular Particle-Continuum Method for Hypersonic, Near Equilibrium Flows," 2010, vol. AIAA 2010-0808.
8. T. R. Deschenes, and I. D. Boyd, *Journal of Thermophysics and Heat Transfer* (Under Review).
9. J. Allegre, D. Bisch, and J. C. Lengrand, *Journal of Spacecraft and Rockets* **34**, 724–728 (1997).
10. T. E. Schwartzentruber, L. C. Scalabrin, and I. D. Boyd, *Journal of Spacecraft and Rockets* **45**, 1196–1206 (2008).